Pertanika J. Sci. & Technol. 31 (1): 33 - 49 (2023)

PERTANIKA JOURNALS

SCIENCE & TECHNOLOGY

Journal homepage: http://www.pertanika.upm.edu.my/

Computational Analysis of Polymer Melt Filling in a Medical Mold Cavity During the Injection Molding Process

Muhammad Khalil Abdullah[1], Mohd Syakirin Rusdi[2]*, Mohd Zulkifly Abdullah[2], Abdus Samad Mahmud[2], Zulkifli Mohamad Ariff[1], Khor Chu Yee[3] and Mohd Najib Ali Mokhtar[4]

[1]School of Materials and Mineral Resources Engineering, Universiti Sains Malaysia, Engineering Campus, 14300 USM, Nibong Tebal, Penang, Malaysia
[2]School of Mechanical Engineering, Universiti Sains Malaysia, Engineering Campus, 14300 USM, Nibong Tebal, Penang, Malaysia
[3]Simulation and Modelling Research Group (SiMMREG), Faculty of Mechanical Engineering Technology, Universiti Malaysia Perlis, 02100 UniMAP, Perlis, Malaysia
[4]Faculty of Manufacturing Engineering, Universiti Teknikal Malaysia Melaka, Hang Tuah Jaya, 76100 Durian Tunggal, Melaka, Malaysia

ABSTRACT

This study describes the results of a mold filling simulation analysis of a medical syringe performed during the thermoplastic injection molding process, which was performed using a computational Fluid Dynamic Simulation (CFD) with the Volume of Fluid Method (VOF). ANSYS Fluent was used for analysis and data collection. Medical grade polypropylene (PP) is considered in this study. The studies consider physical parameters (such as inlet position and syringe thickness) of the injection molding process. The outlet vent must be placed as far away from the inlet as possible to root out entrapped air and allow the molten PP to occupy the mold cavity. The findings revealed that syringe thicknesses ranging from 0.75 mm to 1.00 mm resulted in increased flow velocity, shorter filling time, and faster flow front advancement.

Keywords: Injection molding simulation, medical grade polypropylene, plastic flow, syringe

ARTICLE INFO

Article history:
Received: 17 February 2022
Accepted: 20 June 2022
Published: 19 August 2022

DOI: https://doi.org/10.47836/pjst.31.1.03

E-mail addresses:
mkhalil@usm.my (Muhammad Khalil Abdullah)
syakirin@usm.my (Mohd Syakirin Rusdi)
mezul@usm.my (Mohd Zulkifly Abdullah)
abdus@usm.my (Abdus Samad Mahmud)
zulariff@usm.my (Zulkifli Mohamad Ariff)
cykhor@unimap.edu.my (Khor Chu Yee)
najibali@utem.edu.my (Mohd Najib Ali Mokhtar)
*Corresponding author

ISSN: 0128-7680
e-ISSN: 2231-8526

INTRODUCTION

Despite developing other manufacturing methods and techniques, injection molding is still frequently utilized to create numerous products (Wang et al., 2022; Patil et al., 2021). Intricate forms may be developed using the injection molding method's high pressure (Nagasundaram et al., 2021). Injection molding is now used to make more than one-third of all thermoplastic materials. However, mold fabrication requires a significant amount of time and money. The degree of difficulty is determined by the cavity's design. Additional tooling processes and components are necessary for the complicated shape and distinctive surface cavity. Mold design is typically performed through trial and error, based on years of experience. The fundamental cause and treatment are found via trial and error when a defect develops. If this occurs, the cost and duration of the process, as well as the amount of waste generated by using raw materials, could increase. Due to the high cost of tooling and mold development, conducting a thorough and cost-effective pre-molding analysis is necessary. Alternatively, using simulation modeling tools, the engineer and mold designer may quickly grasp the filling problem and determine the optimal cavity design. Thus, simulations may help accelerate manufacturing and cut testing expenses (Köhn et al., 2021).

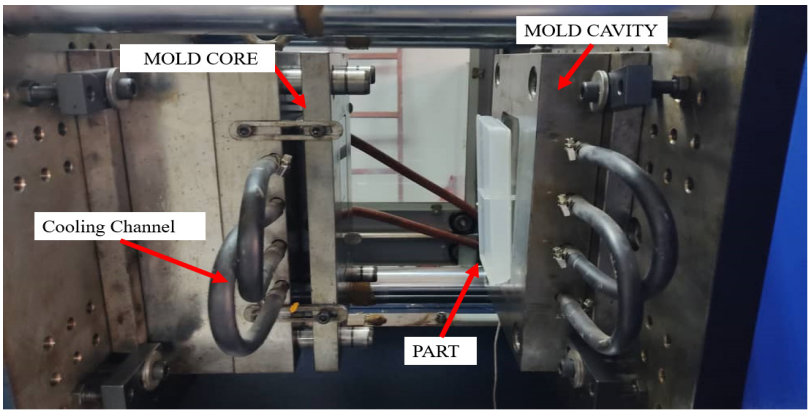

Figure 1. Example of injection molding mold

Rusdi et al. (2016) conducted injection molding simulation using ANSYS FLUENT, the computerized numerical analysis tool for CFD simulation. Injection pressure and temperature were studied. These two process input parameters affect the run time of the mold injection, the advancement of the flow front, and the injection-molding flow.

The ICM process was used in this study by Kwon et al. (2018) for an energy-related application, namely a thin and large polymeric battery case. The mold for the battery case was made using injection molding. The flow of molten polymer into the mold cavity was explored experimentally. To better understand the ICM process, the ICM and traditional injection molding methods were numerically compared. The ICM was determined to

have a low filling pressure, resulting in reduced final product shrinkage and warpage. In addition, the effect of the parting line gap on ICM properties such as filling pressure, filling time, clamping force, warpage, and volumetric shrinkage was investigated using numerical modeling.

A novel constitutive equation for compressing flow, based on the Phan–Thien–Tanner (PTT) model, has been proposed by Cao et al. (2019). This model describes polymers' shear thinning and strain hardening by employing analytical stress solutions for shear and extensional flows. Cao et al. characterize the uniform viscoelastic flow problem for injection/compression in a non-isothermal compressible fluid using a finite element technique. A weak form pseudo-Poisson pressure equation is used to ensure a stable and efficient numerical system. A two-step iterative technique decoupled the velocity, pressure, temperature, and stress. They replicate the benchmark 4:1 contraction flow and compare their results to published findings for validation. Finally, additional injection and compression molding tests are conducted.

Zhang et al. (2019) employed essential microfeatures on a microfluidic flow cytometer chip with a 3:1 aspect ratio as a typical model to establish a suitable approach for describing the filling of the microfeatures using commercial simulation software. Heat transfer coefficients, venting, wall slip, and freeze temperature were all thoroughly researched because they were crucial for micro injection molding but not so for conventional injection molding. A numerical approach for generating material data on thermoset injection molding compounds has been developed by Tran and Gehde (2019), and it has been integrated directly into a simulation program to evaluate its applicability during the thermoset injection molding simulation phase. Also considered during the filling simulation phase was a significant slip phenomenon at the interface of the thermoset melt and the wall surface discovered and observed during injecting molding tests.

Tosello and Costa (2019) did a micro-molding simulation by simulating the real production conditions in the software. Numerous parts of the simulation setup have been investigated to improve the simulation results: the injection rate profile, the injection temperature, the three-mesh specification, and the properties of the molten and solid materials. To make quantitative comparisons, we looked at molding mass, injection pressure, and shot mass. Reducing incidences and uncertainties in experimental data is vital to prevent adding extra uncertainties to simulation computations. Finally, Finkeldey et al. (2020) describe a unique machine learning-based methodology for forecasting the quality attributes of an injection molding process using a mix of simulation and measurement data.

For the low-pressure powder injection molding process, Trad et al. (2020) took an experimental approach of using a cylindrical mold cavity (11.75 mm in diameter and 100 mm long) to validate the numerical modeling of the mold filling stage and component segregation. Autodesk Moldflow Synergy 2019 software was used as a numerical

simulation tool to determine the injected length, filling time, front velocity, shear rate, and pressure, as well as the amount of powder segregation after injection. Aside from that, real measurements of the feedstock's thermal and rheological properties were performed to generate the constitutive equations that would be sent to Moldflow for processing. Finally, a laboratory injection press and real-scale injections (at feedstock temperatures ranging from 80°C to 100°C) were used to validate the findings of the computer models. This study employed a feedstock formulation based on 17–4 PH stainless steel powder (60% vol powder) for experimental characterization and injection.

Trad et al. (2020) were able to duplicate the injection molding process using pvT test equipment and determine the precise fluctuation of a specific volume. There were considerations for the starting temperature and holding pressure, as well as the ending temperature and cooling rate, in addition to the injection temperature and holding time, as well as the cooling rate and holding pressure. Amorphous acrylonitrile-butadiene-styrene (ABS) was used in conjunction with semicrystalline polypropylene (PP). The impact of these parameters on changes in volume during the simulated injection molding cycles was investigated using the design of experiments (DoE) approach.

Sahli et al. (2020) investigated to maximize injection and processing parameters to ensure the molding standard had acceptable properties. Everything of the thermo-rheo-kinetic behavior was determined to accurately predict the entire injection-molding process of curing and cross-linking liquid silicone during the filling stage. Thermal dependence was according to the law of Carreau-Yasuda and Isayev Deng. For the test the thermo-rheo-kinetic behavior and adhesion of liquid silicone during the filling process, Sahli et al. use finite element software (Cadmold 3D).

A collaborative effort between computer scientists, researchers, and technicians has the potential to be critical in the development of simulation software (Khosravani et al., 2022). Effective cooperation is required because of changing client demands and creating new products. This collaboration is possible under specific circumstances, but it is a difficult subject. Despite the many advantages simulation may provide to Industry 4.0, modeling and simulation need further study. The product's geometry, the polymer utilized, the mold, the technical parameters of processing, and the injection molding machine itself all affect the quality of injection molded products (Szabó et al., 2021). Early detection of problems and mold improvement regarding flow simulation can be visualized using simulation models. In this present study, a three-dimensional (3D) mold filling simulation was conducted for the syringe barrel cavity using medical-grade PP material. Additionally, there is a lack of material on the injection molding technique for the medical syringe when medical-grade thermoplastic is used. Thus, this work aims to close this research gap using simulation analysis. The current study made use of CFD software, specifically ANSYS FLUENT 14.0. Rheology experiments were utilized to characterize the rheological properties of PP for use in CFD simulations.

NUMERICAL SIMULATION METHOD

When explaining thermoplastic flow behavior throughout the injection molding process, the Navier-Stokes equations were applied in the current investigation. This approach is reliant on several assumptions, including the following:

- A non-isothermal process
- Constant density
- It is a three-dimensional, laminar, and incompressible flow
- The fluid (molten PP) is Generalized Newtonian Fluid (GNF)

For injection molding simulation analysis, the governing equations of mass, energy, and momentum describe the flow motion of melt thermoplastic in the mold cavity. The mass conservation or continuity equation applies to incompressible flow (Equation 1):

$$\frac{\partial u}{\partial x}+\frac{\partial v}{\partial y}+\frac{\partial w}{\partial z}=0 \tag{1}$$

Conservation of momentum in *i* th direction in an inertial (Equation 2):

$$\frac{\partial}{\partial t}(\rho u_i)+\frac{\partial u}{\partial x_j}(\rho u_i u_j)=-\frac{\partial P}{\partial x_i}+\frac{\partial \tau_{ij}}{\partial x_j}+\rho g_i+F_i \tag{2}$$

where ρ is the fluid density, u is the fluid velocity component, P is the static pressure, τ_{ij} is the viscous stress tensor, and g_i and F_i are the gravitational acceleration and external body force in the i direction, respectively. In the simulation model, the energy equation represents the temperature of the system and fluid. The energy Equation 3 is as follows:

$$\rho c_p\left(u\frac{\partial T}{\partial x}+v\frac{\partial T}{\partial y}+w\frac{\partial T}{\partial z}\right)=k\left(\frac{\partial^2 T}{\partial x^2}+\frac{\partial^2 T}{\partial y^2}+\frac{\partial^2 T}{\partial z^2}\right)+\eta\dot{\gamma} \tag{3}$$

where k is the thermal conductivity, T is the temperature, η is the viscosity, and $\dot{\gamma}$ is the shear rate, respectively.

Viscosity model data is important to simulate molten material (Gou et al., 2011; Koszkul & Nabialek, 2004). The cross model is the most appropriate for describing the rheological behavior of materials during the injection molding process (Hassan et al., 2010; Khor et al., 2010). The cross model describes the shear rate dependency between the Upper Newtonian and Shear-Thinning Regions. The model, also known as the Cross-Exp model, has an exponential (Exp) dependence on temperature. By employing the Cross model with Arrhenius temperature dependency, we suppose that the molten PP is described as GNF (Equations 4 & 5) (Rusdi et al., 2016).

$$\eta(T,\dot{\gamma}) = \frac{\eta_0(T)}{1 + \left(\frac{\eta_0 \dot{\gamma}}{\tau^*}\right)^{1-n}} \tag{4}$$

with

$$\eta_0(T) = B\exp\left(\frac{T_b}{T}\right) \tag{5}$$

τ^* is the parameter that describes the transition region between the power-law region and zero shear rate and of the viscosity curve, η_0 is the zero-shear viscosity, n is the power-law index, B is an exponential-fitted constant, and T_b is a temperature-fitted constant.

Volume of Fluid (VOF) and Boundary Conditions

The VOF model's fundamental principle is to track and locate the fluid-fluid contact. The mold cavity's molten PP and the existing air were two fluid phases during the actual injection molding operation. Therefore, the VOF approach detects and creates the liquid phase distribution. This approach assigns a scalar (f) to each cell in the computational grid that shows what fraction of the cell's volume is occupied by liquid (Malgarinos et al., 2014). Thus, when the cell contains only molten PP, the value of f equals one ($f = 1$), when the cell contains no molten PP (or air), the value of f equals zero ($f = 0$), and when the value is between 0 and 1 ($0 < f < 1$), the cell comprises "interface" cells, also known as the molten PP front. The equation of the melt front with time was determined by the following transport Equation 6:

$$\frac{dF}{dt} = \frac{\partial F}{\partial t} + \nabla \cdot (uf) = 0 \tag{6}$$

The simulation defined molten PP and air as two different fluid phases. While the molten PP fills the cavity during injection, air escapes through the outlet valves. VOF monitored the filling of the melted plastic and the progression of the flow front over time. In the post-processing step, the mobility of molten PP may be viewed. The computational domain of the CFD analysis was defined by the inlet, outlet, and wall boundaries. The boundary conditions defined on the 3D model are depicted in Figure 1. The following are the boundaries and initial conditions:

a) On mold wall: $u = v = w = 0$; $T = T_w$

b) On melt front: $p = 0$

c) At inlet: $p = p_{in}(x, y, z)$; $T = T_{in}$

Modeling and Mesh Development

SOLIDWORKS software was used to make the model of the medical syringe (Figure 2). The syringe model is considered the cavity in the real injection molding mold. The outer surface of the model is considered the mold wall. The syringe's specifications have a thickness of 0.25 mm, 0.50 mm, 0.75 mm, 1.00 mm, and 1.25 mm. The CFD computational domain was established in ANSYS WORKBENCH based on the dimensions. The mold entry is positioned on the syringe barrel's body, while the air vent is on the syringe barrel's tip. These locations determined the computational domain's inlet and outflow bounds. The syringe cavity is positioned on the y-axis during the injection molding, and molten PP plastic is injected from the inlet (z-axis). Once the model has been exported to ANSYS WORKBENCH, the model will be meshed (Figure 3), applying boundary conditions (such as inlet, outlet, and wall), creating and performing simulations. LyondellBasell 6331 (LB6331) medical-grade polypropylene was used in this investigation, and rheological characterization data were gathered by capillary rheometer experimental work using the GÖTTFERT Rheograph 25 (capillary rheometer machine).

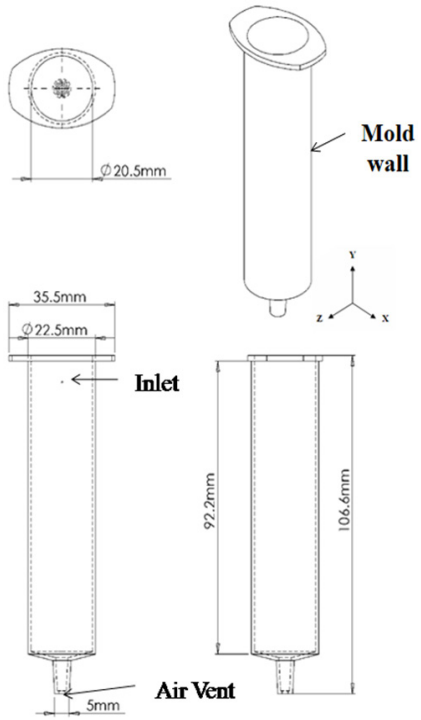

Figure 2. Dimensions and boundary conditions of the syringe barrel mold cavity

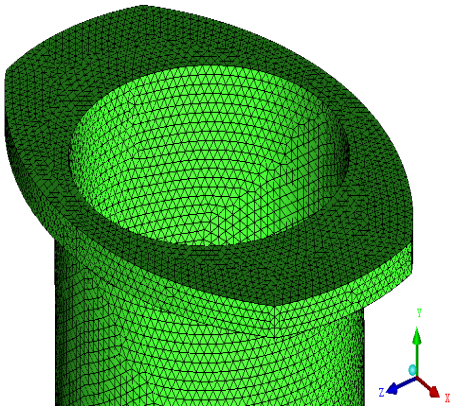

Figure 3. 3-D meshed model for syringe barrel mold cavity

RESULTS AND DISCUSSION

Effect of Barrel Thickness for Syringe Barrel Cavity

Cavity thickness is one of the characteristics that affect how molten PP flows.The influence of cavity thickness on velocity profile, flow front advancement, and filing time will be discussed in this section. The thickness ranges between 0.25 mm and 1.25 mm and is

only evaluated for the syringe's thickness up to the tip. The thickness of the flange remains constant. This investigation used a constant system pressure of 5 MPa and a constant melt temperature of 190°C.

Filling Time. In Figure 4, a fixed point (Point 1) is depicted in the vicinity of the outlet region. This observation is being made to keep an eye out for the existence of molten PP in the outflow zone. The mold is deemed full when this spot exhibits continuous maximum pressure.

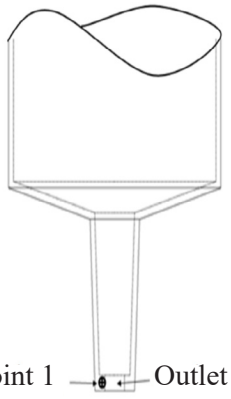

Figure 4. Point where the pressure value was taken

As illustrated in Figure 5, case 0.25 mm could not fill the cavity due to the absence of a maximum pressure plot compared to other thicknesses. The first case fills in 3.99 seconds, followed by case 1.00 mm (4.46 seconds), case 1.25 mm (5.21 seconds), and lastly, the last case 0.5 mm (6.99s), as depicted in Figure 6. When looking at the pressure distribution, the 1.25 mm size had the highest pressure, followed by 1.00 mm, 0.75 mm, and 0.5 mm for the following three sizes, respectively. A bigger thickness results in a greater maximum pressure, according to the study's results. Because a thick cavity space has a lower barrier to flow and a smaller pressure loss than a thin cavity space, molten polypropylene (PP) may easily fill the gap during the injection molding process. When the system pressure was 5 MPa, and the temperature was 190°C, it was discovered that the molten polypropylene did not have enough energy to fill the cavity gap of Case 0.25 mm in this investigation. Figure 5 illustrates this behavior. At 9 seconds of filling time, the pressure in the 0.25 mm casing is still quite low compared

Flow Front Advancement. According to Figure 7, the advancement of the molten PP's flow front was estimated by creating a line in the simulation model (depicted as the red dotted line in Figure 7) through the center of the syringe cavity on the inlet side and the flow front was measured starting from the inlet.

Figure 8 depicts the advancement of the flow front at various thicknesses. Molten polypropylene (PP) in a syringe barrel with a thin cavity flows faster than molten polypropylene in a syringe barrel with a thick cavity at an early stage (0.5s). The flow was close to the entrance when minimal pressure and volumetric loss were critical. Reduced cavity volume necessitates a shorter filling time (rapid filling process) and faster flow front

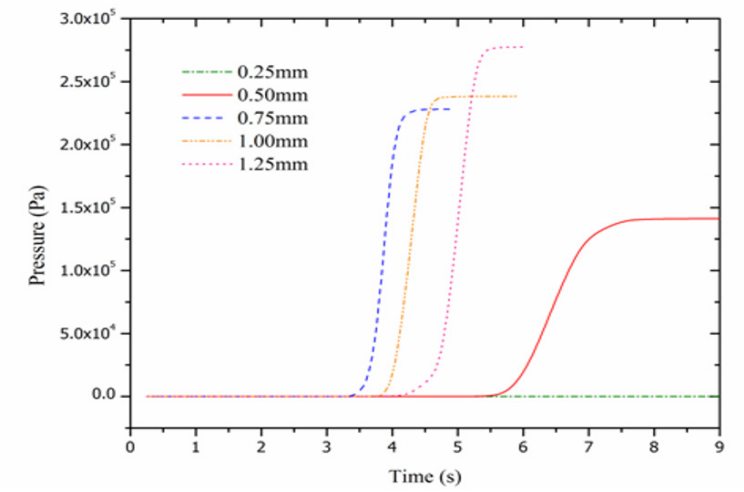

Figure 5. Pressure distribution for different thicknesses

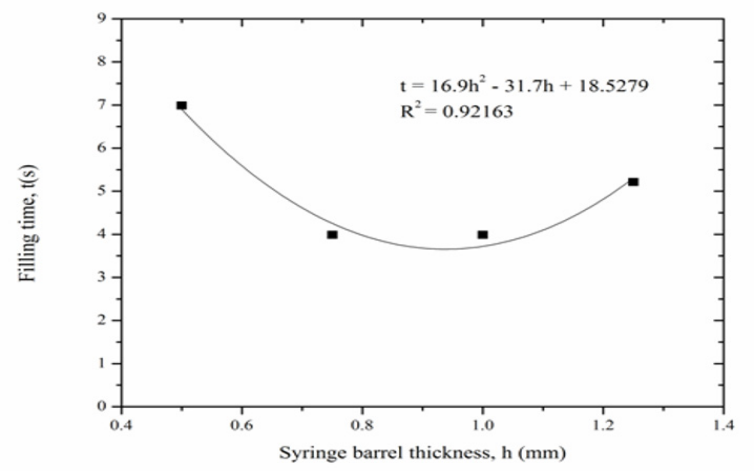

Figure 6. Filling time for different syringe barrel thicknesses

advancement. Because the thick syringe cavity has a larger capacity to fill, the flow front progress is slower than with a narrow cavity. Throughout the filling process, case 0.25 mm flow front advancement becomes slower and practically static, and molten PP ceases to flow into the cavity (Figure 9). The 0.25 mm thickness results in increased flow resistance, which results in increased pressure loss until the pressure is no longer sufficient to propel the flow. However, the thick cavity's flow front advances smoothly as time passes. At this point, two things are considered: pressure loss and the volume to be filled with air. In addition to having less pressure loss, a thicker cavity also has a larger volume than the melt flow must occupy, as opposed to a thinner cavity. As a result, case 0.75 mm has the fastest

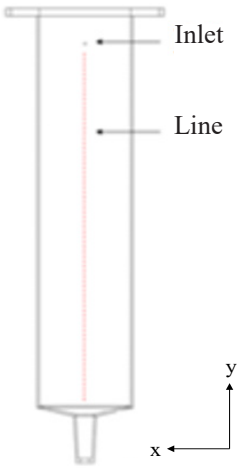

Figure 7. The line for flow front advancement measurement

flow front advancement despite having a greater pressure loss than cases 1.00 mm and 1.25 mm, despite having a higher-pressure loss than the other cases. 0.75 mm thickness provides the best balance between pressure loss and the occupied syringe barrel volume, resulting in the fastest fill time and flow front advancement.

Velocity. During the injection molding process, it is difficult to determine the velocity of the molten PP. As a result, the simulation modeling method is critical in providing engineers with a realistic process

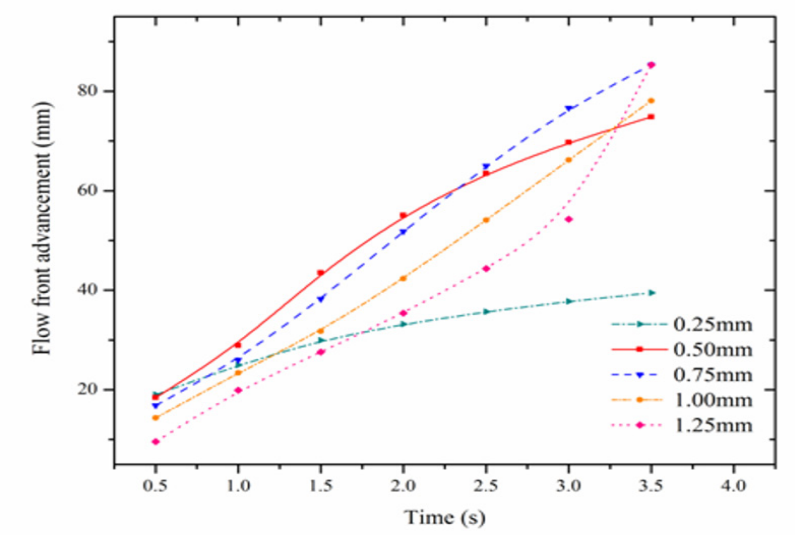

Figure 8. Flow front advancement for different thicknesses

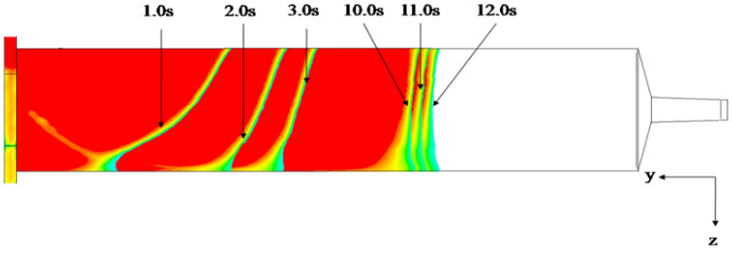

Figure 9. Flow front advancement of case 0.25mm

picture. Additionally, it assists the engineer in comprehending the flow behavior and flowability of the part design. The velocity values of molten PP are estimated at eight sites in this investigation, as seen in Figure 10. The eight locations are positioned 10mm below the inlet (-y-direction).

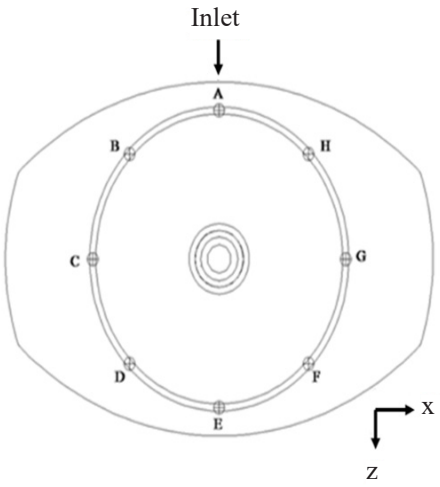

Figure 10. Point where the velocity values were taken

The velocity values for various thicknesses at 2s are displayed in Figure 11. According to expectations, the fastest velocity is found in the thickest layer (0.75mm), which can be found in all locations. In contrast, case 1.25 mm has the highest value at point E due to its smaller size. Furthermore, since Point E is located at the intersection of two directions of flow, it is considered an extreme velocity point since the value was obtained at the point where the two directions of flow meet, resulting in a high flow velocity at the intersection of Point E (Figure 12).

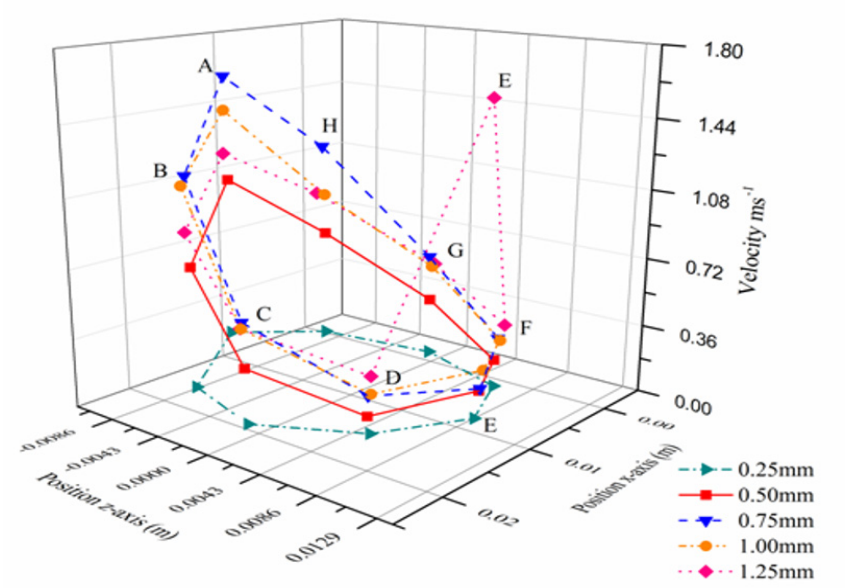

Figure 11. Velocity values for different thicknesses at 2s

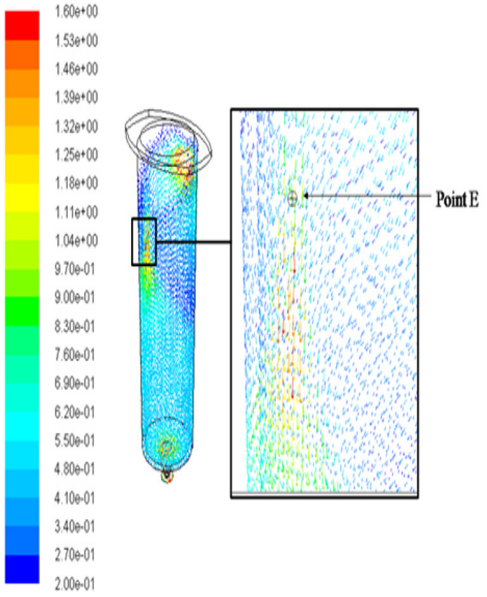

Figure 12. Velocity vector (unit:ms^{-1}) at point E for Case 1.25 mm at 2s

As a result, in each example, the highest velocity values were obtained at normal flow at point A. In Figure 13, the greatest velocities were tabulated. A negative quadratic trend can be observed between 0.75 mm and 1.0mm in terms of maximum velocity. The velocity will be extremely low unless the cavity thickness is more than this range. When using 0.75 mm thick syringe cavities, the case 0.75 mm has the highest velocity figures, suggesting that it will fill the syringe the quickest and advance the flow front the fastest. While it has a lower maximum pressure (and therefore more pressure loss) than the 1.00 mm and 1.25 mm, the smaller cavity volume benefits from, the higher velocity profile due to the smaller cavity capacity.

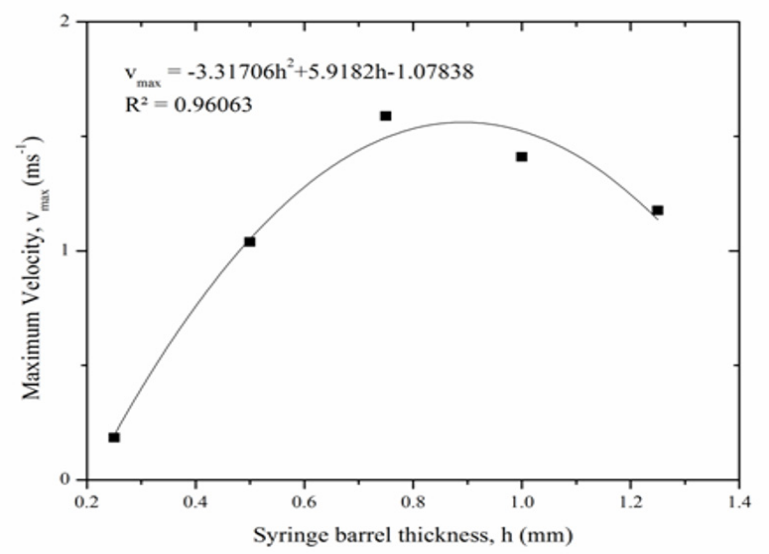

Figure 13. Maximum velocity for different barrel thicknesses

Effect of Inlet Position for Syringe Barrel Cavity

When the syringe barrel is injection molded, the inlet site is often positioned in the syringe body. Therefore, the location of the inlet was changed in the same y-axis line at five different

locations along this section. The points are located at distances of 6.5 mm to 86.5 mm from the flange, with a 20mm distance between each point. The melt temperature and system pressure were maintained at 5 MPa and 190°C, respectively.

Cavity Filling. In order to determine the amount of pressure applied during the injection molding process, two points were used in the experiment. Point 1 was placed closer to the exit, as described in Figure 4, and Point 2 was placed closer to the syringe barrel flange, as illustrated in Figure 14. The first point was used to detect the presence of molten PP in the bottom portion of the syringe cavity, while the second point was utilized to detect the presence of molten PP in the top area of the syringe cavity (flange section). The mold is deemed filled when these spots exhibit the same maximum pressure.

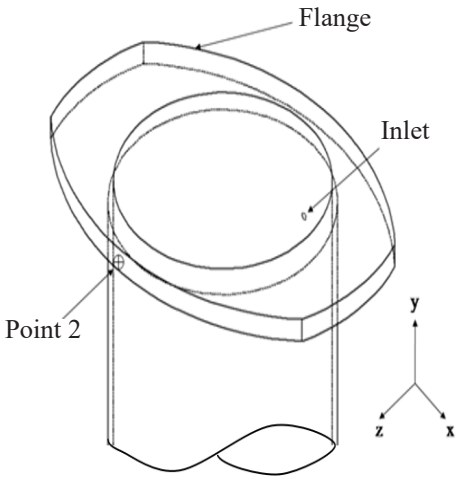

Figure 14. Point 2 location at screw barrel mold cavity

Only the pressures of cases 6.5 mm, 46.5 mm, and 86.5 mm can reach point 1 (Figure 15). However, only case 6.5 mm reached the highest constant pressure curve at point 2 (Figure 16). Based on these two observations, only the case 6.5 mm inlet position can fill the syringe barrel cavity. In other instances, those who were unable to reach one or both locations were deemed to have failed to fill the cavity. The results indicated that the filling of case 86.5 mm with molten PP can only reach point 1 due to its proximity to the outlet and point 1. Its placement also results in unusually high-pressure values when it reaches point 1 at approximately 11.45 MPa, as opposed to 0.14 MPa and 0.18 MPa for cases 6.5 mm and 46.5 mm, respectively.

Flow Front Advancement. When five various intake positions are used, only case 6.5 mm fills the cavity, according to the simulation findings. This experiment considered just one exit while designing the syringe barrel cavity. The other examples encountered difficulties because trapped air at the flange part impeded the flow of molten PP. When the molten PP flow from the input side merged with the flow from the backside of the mold cavity, the molten PP flow ceased (Figure 17). The merge entrapped air around the upper side of the cavity (flange portion), preventing it from exiting through the outlet. Even though molten PP does not reach point 2 in cases 26.5 mm, 46.5 mm, and 66.5 mm, these three instances

retain a high-pressure value at point 2 (Figure 16). The pressure values were determined by the pressure of trapped air within the flange section, which prevents the molten PP from filling the flange section.

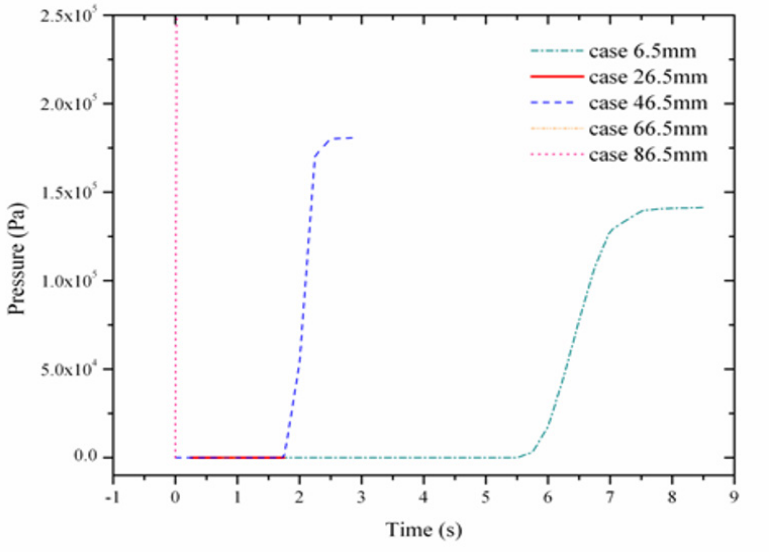

Figure 15. Pressure distribution at point 1

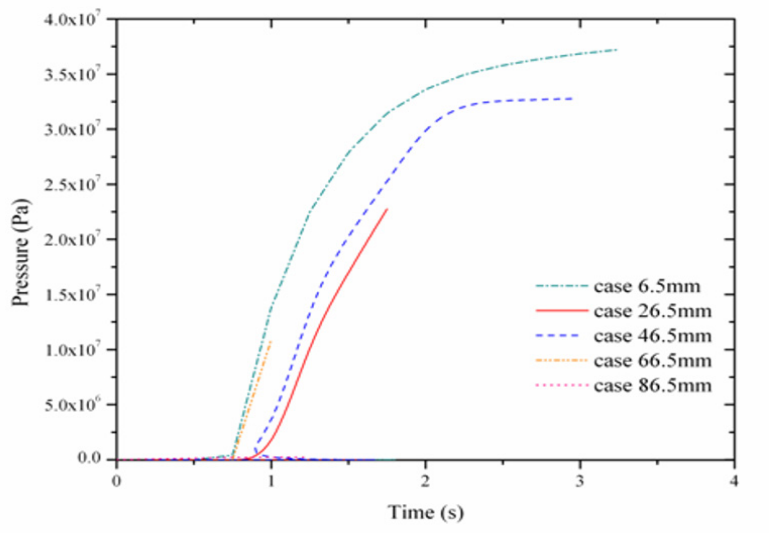

Figure 16. Pressure distribution at point 2

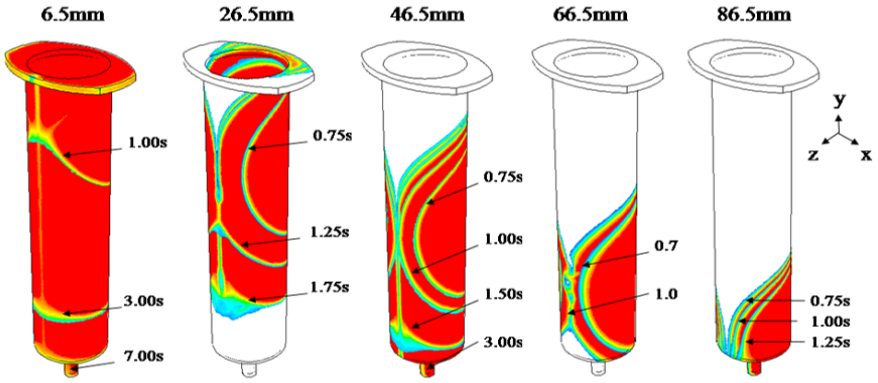

Figure 17. Flow front advancement for different inlet positions

The simulation findings demonstrated that intake position influences pressure and flow front advancement. Additionally, the cavity exit position is crucial for injection molding the syringe barrel. An insufficient exit would result in air entrapment and act as a barrier to the molten PP filling that region. Therefore, it is recommended that the outlet be situated as far away from the intake as practicable. The injection molding procedure must take the output location into account. The outlet is critical for venting air from the mold cavity and facilitating the filling of the cavity with molten PP.

CONCLUSION

CFD simulations of the syringe barrel were performed, and the barrel was filled with medical-grade PP (LB6331). An appropriate outlet placement must be considered for the injection molding process to be successful. The exit must be as far away from the inlet as possible to properly channel out air and give space for the molten PP to occupy the hollow area. Syringe barrels of varying thickness (0.25 mm, 0.5 mm, 0.75 mm, 1.00 mm and 1.25 mm) exhibit varying flow characteristics. The right thickness must be determined carefully and not simply based on whether a thicker or thinner thickness is acceptable. While thinner thickness results in greater pressure losses than higher thickness, thinner thickness requires less volume to occupy. The range of 0.75 mm to 1.00 mm demonstrated a faster filling time, a faster advancement of the flow front, and a greater flow velocity in the current investigation. These results demonstrated that CFD simulation could simulate capable of simulating the syringe barrel injection molding process.

ACKNOWLEDGEMENT

The authors acknowledge the support from the Short-Term Research Grant, Universiti Sains Malaysia (304/PMEKANIK/6315569) and the School of Mechanical Engineering, Universiti Sains Malaysia.

REFERENCES

Cao, W., Shen, Y., Wang, P., Yang, H., Zhao, S., & Shen, C. (2019). Viscoelastic modeling and simulation for polymer melt flow in injection/compression molding. *Journal of Non-Newtonian Fluid Mechanics, 274*, Article 104186. https://doi.org/10.1016/j.jnnfm.2019.104186.

Finkeldey, F., Volke, J., Zarges, J. C., Heim, H. P., & Wiederkehr, P. (2020). Learning quality characteristics for plastic injection molding processes using a combination of simulated and measured data. *Journal of Manufacturing Processes, 60*, 134-143. https://doi.org/10.1016/j.jmapro.2020.10.028.

Gou, G., Xie, P., Yang, W., & Ding, Y. (2011). Online measurement of rheological properties of polypropylene based on an injection molding machine to simulate the injection-molding process. *Polymer Testing, 30*(8), 826-832. https://doi.org/10.1016/j.polymertesting.2011.08.005.

Hassan, H., Regnier, N., Pujos, C., Arquis, E., & Defaye, G. (2010). Modeling the effect of cooling system on the shrinkage and temperature of the polymer by injection molding. *Applied Thermal Engineering, 30*(13), 1547-1557. https://doi.org/10.1016/j.applthermaleng.2010.02.025.

Khor, C. Y., Ariff, Z. M., Ani, F. C., Mujeebu, M. A., Abdullah, M. K., Abdullah, M. Z., & Joseph, M. A. (2010). Three-dimensional numerical and experimental investigations on polymer rheology in meso-scale injection molding. *International Communications in Heat and Mass Transfer, 37*(2), 131-139. https://doi.org/10.1016/j.icheatmasstransfer.2009.08.011.

Khosravani, M. R., Nasiri, S., & Reinicke, T. (2022). Intelligent knowledge-based system to improve injection molding process. *Journal of Industrial Information Integration, 25*, Article 100275. https://doi.org/10.1016/j.jii.2021.100275.

Köhn, C., van Laethem, D., Deconinck, J., & Hubin, A. (2021). A simulation study of steric effects on the anodic dissolution at high current densities. *Materials and Corrosion, 72*(4), 610-619. https://doi.org/10.1002/maco.202012051.

Koszkul, J., & Nabialek, J. (2004). Viscosity models in simulation of the filling stage of the injection molding process. *Journal of Materials Processing Technology, 157*(2), 183-187. https://doi.org/10.1016/j.jmatprotec.2004.09.027.

Kwon, Y. I., Lim, E., & Song, Y. S. (2018). Simulation of injection-compression molding for thin and large battery housing. *Current Applied Physics, 18*(11), 1451-1457. https://doi.org/10.1016/j.cap.2018.08.017.

Malgarinos, I., Nikolopoulos, N., Marengo, M., Antonini, C., & Gavaises, M. (2014). VOF simulations of the contact angle dynamics during the drop spreading: Standard models and a new wetting force model. *Advances in Colloid and Interface Science, 212*, 1-20. https://doi.org/10.1016/j.cis.2014.07.004.

Nagasundaram, N., Devi, R. S., Rajkumar, M. K., Sakthivelrajan, K., & Arravind, R. (2021). Experimental investigation of injection moulding using thermoplastic polyurethane. *Materials Today: Proceedings, 45*, 2286-2288. https://doi.org/10.1016/j.matpr.2020.10.264.

Patil, D. C., Kelageri, N. K., Janawade, S. A., & Mishrikoti, M. S. (2021). Design and analysis of 25 T injection molding machine. *Materials Today: Proceedings, 46*, 2596-2601. https://doi.org/10.1016/j.matpr.2021.02.262.

Rusdi, M. S., Abdullah, M. Z., Mahmud, A. S., Khor, C. Y., Aziz, A., Ariff, Z. M., & Abdullah, M. K. (2016). Numerical investigation on the effect of pressure and temperature on the melt filling during injection molding process. *Arabian Journal for Science and Engineering, 41*(5), 1907-1919. https://doi.org/10.1007/s13369-016-2039-0.

Sahli, M., Barriere, T., & Roizard, X. (2020). Experimental and numerical investigations of bi-injection moulding of PA66/LSR peel test specimens. *Polymer Testing, 90*, Article 106748. https://doi.org/10.1016/j.polymertesting.2020.106748.

Szabó, F., Suplicz, A., & Kovács, J. G. (2021). Development of injection molding simulation algorithms that take into account segregation. *Powder Technology, 389*, 368-375. https://doi.org/10.1016/j.powtec.2021.05.053.

Tosello, G., & Costa, F. S. (2019). High precision validation of micro injection molding process simulations. *Journal of Manufacturing Processes, 48*, 236-248. https://doi.org/10.1016/j.jmapro.2019.10.014.

Trad, M. A. B., Demers, V., Côté, R., Sardarian, M., & Dufresne, L. (2020). Numerical simulation and experimental investigation of mold filling and segregation in low-pressure powder injection molding of metallic feedstock. *Advanced Powder Technology, 31*(3), 1349-1358. https://doi.org/10.1016/j.apt.2020.01.018.

Tran, N. T., & Gehde, M. (2019). Creating material data for thermoset injection molding simulation process. *Polymer Testing, 73*, 284-292. https://doi.org/10.1016/j.polymertesting.2018.11.042.

Wang, J., Hopmann, C., Kahve, C., Hohlweck, T., & Alms, J. (2020). Measurement of specific volume of polymers under simulated injection molding processes. *Materials & Design, 196*, Article 109136. https://doi.org/10.1016/j.matdes.2020.109136

Zhang, H., Fang, F., Gilchrist, M. D., & Zhang, N. (2019). Precision replication of micro features using micro injection moulding: Process simulation and validation. *Materials & Design, 177*, Article 107829. https://doi.org/10.1016/j.matdes.2019.107829.